The radial electric field dynamics in the neoclassical plasmas

S. V. Novakovskii, C. S. Liu, and R. Z. Sagdeev
Institute for Plasma Research, University of Maryland, College Park, Maryland 20742-3511

M. N. Rosenbluth
University of California at San Diego, La Jolla, California

(Received 15 April 1997; accepted 16 September 1997)

A numerical simulation and analytical theory of the radial electric field dynamics in low collisional tokamak plasmas are presented. An initial value code ''ELECTRIC'' has been developed to solve the ion drift kinetic equation with a full collisional operator in the Hirshman–Sigmar–Clarke form together with the Maxwell equations. Different scenarios of relaxation of the radial electric field toward the steady-state in response to sudden and adiabatic changes of the equilibrium temperature gradient are presented. It is shown, that while the relaxation is usually accompanied by the geodesic acoustic oscillations, during the adiabatic change these oscillations are suppressed and only the magnetic pumping remains. Both the collisional damping and the Landau resonance interaction are shown to be important relaxation mechanisms. Scalings of the relaxation rates versus basic plasma parameters are presented. © *1997 American Institute of Physics.* [S1070-664X(97)03312-0]

I. INTRODUCTION

The radial electric field dynamics and closely related phenomena of the poloidal and toroidal rotation of tokamak plasmas have been of considerable interest. In particular, the build-up of the transport barrier, and the improvement of plasma confinement have been attributed to the generation of the radial electric field. The most striking evidences are related to the famous low to high (L-H) transition in tokamaks,[1] and the recently discovered regimes of the enhanced reversed shear (ERS) experiments[2] and negative center shear (NCS) experiments.[3] In all of these cases the formation of the transport barrier, which takes place in the edge region for the L-H transition, and in the core plasmas for the ERS and NCS discharges, could be explained by means of the radial electric field generation. This electric field, existing in the region of the sharp pressure gradients, produces the $\mathbf{E}\times\mathbf{B}$ flow with a shear, which in turn has a strong stabilizing influence on the plasma turbulence.[4,5] The origin of the radial electric field can be of complicated nature. Several theoretical mechanisms of such ''spin-up'' have been proposed, in particular due to the Reynolds stress,[6] the ion orbit loss effect,[7] and the Stringer–Hassam poloidal asymmetric driving force.[8,9] Usually these models exploit some particular aspects of the plasma edge parameters, turbulence, instabilities, etc. However, there has for a long time been known a universal mechanism of the radial electric field generation, discovered by Sagdeev and Galeev,[10] due to the intrinsic non-ambipolarity of the non-equilibrium neoclassical plasmas. Namely, in the plasmas with density and temperature gradients, an initially Maxwellian distribution inevitably evolves into a state with a finite radial electric field. It has also been realized that this evolution towards the neoclassical equilibrium depends strongly on the plasma collisionality.

The goal of this paper is to study analytically and numerically the problems related to this evolution, including determination of the steady-state values of the radial electric field and temporary rates of evolution. Our major objective is to create a unified picture of evolution in high and low collisional plasmas and to find equilibrium distributions and flows. It is important to understand that even the equilibrium $\mathbf{E}\times\mathbf{B}$ flow can only be determined from the solution of the non-steady-state problem. Hirshman[11] showed that the neoclassical equilibrium is reached through a complicated process involving the viscous damping of the poloidal rotation and the generalized angular momentum conservation in the axisymmetric systems.

Let us recapitulate briefly the results devoted to the neoclassical equilibrium in the tokamak plasmas. Three neoclassical collisional regimes can be distinguished.[12–16] As usual we consider two characteristic time units: first, $\tau_b = qR/v_T$ the ion bounce or transit time, where R is the major radius of a torus, q is a safety factor, and $v_T=(2T/m)^{1/2}$ the thermal velocity, and, second, $\tau_i = 1/\nu_{ii}$ where ν_{ii} is the ion–ion collisional frequency. The collisional, or Phirsch–Schluter (PS) regime, is characterized by $\nu_{ii} \gg \omega_b$, where the bounce frequency is given by $\omega_b = 1/\tau_b$. In this situation the regular particle orbits in a torus are destroyed by collisions and a fluid approximation can be used. For weaker collisions $\nu_{ii}\tau_b \leqslant 1$ transit or circulating orbits exist, which correspond to the plateau regime. Finally, for very weak collisions, $\nu_{ii}\tau_b \leqslant \epsilon^{3/2}$, where the inverse aspect ratio $\epsilon = r/R$ is less than unity, and r is the minor radius of a torus, both circulating and trapped (''bananas'') orbits exist, and this is the case of the ''banana'' regime. A dimensionless parameter, conveniently describing the transition from the banana to plateau regime, is $\nu_* = \nu_{ii}\tau_b/\epsilon^{3/2}$, such that $\nu_* \leqslant 1$ corresponds to the banana regime. In spite of necessity of the kinetic approach in the plateau and banana regime, it was shown that a steady-state is conveniently described by a following fluid formula, given by Hazeltine,[17] which relates the equilibrium poloidal velocity to the temperature gradient diamagnetic velocity: $U_\theta = kV_T$, where $U_\theta = \Theta\overline{U_{||}} + V_E + V_n + V_T$. In this equation, $U_{||}$ is the equilibrium parallel velocity, and $\overline{U_{||}}$ is its poloidally average part, Θ is the ratio of the poloidal magnetic field to the toroidal one, V_E is the $E\times B$ velocity

 1070-664X/97/4(12)/4272/11/$10.00

given by $V_E=-cE_r/B$, and the diamagnetic velocities are given by $V_T=cT/(eBL_T)$ and $V_n=cT/(eBL_n)$. Here $L_n=d\ \ln n/d\ln r$ and $L_T=d\ \ln T_i/d\ln r$ have the meaning of the inverse density and ion temperature gradient lengths. The coefficient k depends on the plasma collisionality. It equals -2.1 in the PS regime, -0.5 in the plateau regime and 1.17 in the banana regime. In spite of its simplicity this formula does not determine explicitly the electric field and $U_{||}$ and the consideration of the temporal evolution is required.[17]

Several papers have been devoted to the solution of the non-steady-state neoclassical problem.[18–28] This problem can be formulated as follows: suppose we have a tokamak plasma with a local Maxwellian (or some other non-equilibrium in the neoclassical sense!) distribution, which has the radial temperature and density gradients, and some initial (zero, for simplicity) radial electric field. How long does take to reach the neoclassical equilibrium, and what are the electric field and the distribution (in particular $U_{||}$ velocity) at the end of the relaxation? Hassam and Kulsrud[22] have studied the PS regime, the only case where the fluid description is possible. It has been found that the relaxation is described by a symbolic equation for the poloidal velocity:

$$\partial U_\theta/\partial t=-\nu_{MP}(U_\theta-kV_T), \tag{1}$$

where $k=k_{PS}=-2.1$, and the so-called magnetic pumping frequency is given by $\nu_{MP}=\nu_{PS}\cong\nu_b^2/\nu_{ii}$. The solution to this equation, written in terms of the drift velocity V_E, can also be presented as

$$V_E=V_{E\infty}+A\ \exp(-\gamma_{MP}t), \tag{2}$$

where the relaxation parameter γ_{MP} is given by $\gamma_{MP}=\nu_{PS}$, and the equilibrium velocity $V_{E\infty}$ is controlled by the initial condition.

For the lower collisional regimes, plateau and banana, the situation is more complicated. Technically the problem lies in calculating the parallel plasma viscosity. It has been realized that a ''quasi-static'' viscosity (see, e.g., Refs. 21, 22) cannot provide a proper evolution picture, since it was shown that the viscosity (where we speak about the so-called parallel viscosity, resulting form the pressure anisotropy) depends on the non-stationary terms like $\partial V_E/\partial t$, which is a manifestation of the enhanced polarization current in the tokamak plasma. The kinetic treatment of the problem has been proposed in several papers.[23–28] Almost each of these papers either derives a corresponding ''fluid-like'' equation (1) for U_θ or (2) for V_E dynamics, or numerically calculates eigenfrequencies of such evolutionary equations. In particular, several different scalings for γ_{MP} have been proposed in the banana regime: $\nu_{ii},\nu_{ii}/\epsilon^{1/2},\nu_{ii}/\epsilon$. The important common feature of these approaches is the collisional (in the fluid sense) nature of the relaxation. For very low collisional regions it leads to a situation, where the characteristic time of relaxation is much longer than the corresponding transit time, $\gamma_{MP}\ll\omega_b$. Technically, it corresponds to a special ordering, such that $\partial/\partial t\ll\omega_b$ in the process of solving the drift kinetic equation; see, e.g., Refs. 24, 25.

If this ordering is not used and fast processes with $\partial/\partial t\approx\omega_b$ are allowed, then there exists an additional branch of plasma waves, discovered by Winsor, Johnson and Dawson,[29] and called the Geodesic Acoustic Mode (GAM). This mode is characterized by oscillations of the plasma column in the vertical direction with a characteristic frequency $\omega_{GAM}\approx V_T/R$. Hassam and Drake[30] derived a cubic symbolic equation, describing a coupling of this GAM mode with a magnetic pumping mode [see Eqs. (1)–(2)], and discussed some general properties of the resulting solution. For the later purpose, we shall present such a solution symbolically as

$$V_E=V_{E\infty}+A\ \exp(-\gamma_{MP}t)+B\ \cos(\omega_{\mathrm{GAM}}t+\phi)\times\exp(-\gamma_{\mathrm{GAM}}t), \tag{3}$$

where ϕ is a phase factor. Recently Lebedev *et al.*[31] considered a relaxation in the plateau regime. Most of Ref. 31 is devoted to a pure collisionless case. It has been shown that if the resonance condition is satisfied, $\omega_b=\omega_{\mathrm{GAM}}$, then there exists a strong collisionless, Landau-like damping mechanism. Remarkably, this mechanism depends strongly upon the value of the plasma safety factor q. Indeed given $\omega_b=V_T/qR$, and $\omega_{\mathrm{GAM}}=\zeta V_T/R$, where ζ is of the order of unity, the resonant condition yields $q=1/\zeta\approx1$. In such a situation the results of Ref. 31 in the limit $\nu_{ii}\to0$ can be interpreted as follows. The third term in the right hand side of Eq. (3) is decayed with $\gamma_{\mathrm{GAM}}\approx\omega_b$. Reference 31 also provides some insight as to what happens if the resonance condition is not satisfied, which is the case when $q>>1$. It also contains the effects of small, but finite collisions. It is important to bear in mind, however, that the general case of Eq. (3), i.e. when all the three terms are present, has not been considered in Ref. 31. Namely, the conventional magnetic pumping term [second in Eq. (3)] has been neglected. Thus, the results of Ref. 31, corresponding to the ''non-resonant'' case with finite collisions can be interpreted as $\gamma_{\mathrm{GAM}}\approx\nu_{ii}$.

In this paper we perform a direct numerical study of the electric field dynamics in the neoclassical plasmas. For this purpose we have developed a numerical code ''ELECTRIC.'' This code solves the ion drift kinetic equation with a full collisional term in the Hirschman–Sigmar–Clarke[32] form, and a quasineutrality equation. This form of the collisional operator makes it possible to consider each collisional regime, and hence to obtain a unified picture of the relaxation. ''ELECTRIC'' is an initial value code, it calculates the evolution of the distribution function $f(v,z,\theta,t)$, where $z=v_{||}/v$ is the pitch-angle, and the radial electric field drift $V_E(t)$. The ultimate purpose of the paper is to study the general relaxation scenario, given by Eq. (3), and to determine the relaxation rates γ_{MP} and γ_{GAM}. The next important issue is related to different mechanisms of ''preparing'' the plasma system. Namely, at least two possible types of switch-on can be considered. First one corresponds to a sudden switch-on, and can be realized, for example, by the choice of the zero initial electric field and the initial distribution function, taken to be a local Maxwellian with given temperature and density gradients. This case, which we will refer as ''standard,'' is more general in the sense of Eq. (3), since all three modes take off. In a real experimental situation this case looks unlikely, except for the discharges with very fast disruptions, such that the pressure profile is changed for less than the collisional time. Another case corresponds to an adiabatic switch-on. For example, once a steady state is reached after a complete evolution of the ‘‘standard’’ case, one slowly varies the temperature or density gradients. If it is done slower than the GAM oscillatory time, or simply speaking, the ion transit time, then the GAMs would not take off at all, and one is left with a pure magnetic pumping relaxation. This ‘‘soft’’ switch-on can also be considered as closer to a real experimental situation during the neutral beam heating, performed, for example, in a Tokamak Fusion Test Reactor (TFTR) or DIII-D plasma (see Refs. 2, 3, 5 for more detail on the neutral beam heating).

Accordingly, Section II of the paper is devoted to formulation of the problem and derivation of the basic equations. In Section III the results of the numerical simulation are presented. There we start from the ‘‘standard’’ case. We demonstrate here resonant and non-resonant scenarios of the relaxation. Next we consider the ‘‘soft’’ switch-on. We present both resonant and non-resonant cases in the banana and plateau regimes. We also discuss ϵ dependence of the relaxation rates γ_{MP} and γ_{GAM}. In Section IV we discuss the fluid approximation and some general properties of relaxation, following from the incompressibility and conservation of the generalized toroidal angular momentum. In Section V we briefly discuss the collisional damping of the geodesic acoustic oscillations. Finally Section VI is devoted to discussion and conclusions.

II. BASIC EQUATIONS

We consider a simple axisymmetric tokamak with the magnetic field, given by $\mathbf{B}=B_0(\mathbf{e}_\zeta+\Theta\mathbf{e}_\theta)/(1+\epsilon\cos\theta)$, where ζ and θ are the toroidal and poloidal angles of a torus, respectively. The poloidal angle θ is chosen such that $\theta=0$ corresponds to the outboard of a torus. The inverse aspect ratio $\epsilon=r/R$ is assumed to be small. The major radius is given by $R=R_0+r\cos\theta$, where r is the minor radius. The ion distribution function f depends on the total velocity of a particle v, its parallel velocity $v_{||}$. It is also considered to be a function of θ and r. The electric field is described by the electrostatic potential $\phi(r,\theta,t)=\phi_0(r,t)+\phi_1(r,\theta,t)$. For simplicity we will neglect the part ϕ_1 in this paper, thus only the radial electric field $E_r(r,t)=-d\phi_0(r,t)/dr$ will be studied. For the function $f(v,v_{||},\theta,r)$ we have a drift kinetic equation, given by

$$\frac{\partial f}{\partial t}+(\Theta v_{||}+V_E)\frac{\partial f}{r\partial\theta}+\frac{dv_{||}}{dt}\frac{\partial f}{\partial v_{||}}+\frac{dv^2/2}{dt}\frac{\partial f}{\partial v^2/2}+V_r\frac{\partial f}{\partial r}=St(f), \tag{4}$$

where the radial drift velocity is:

$$V_r=-\frac{v_{||}^2+v^2}{2\omega_B R}\sin\theta-\frac{1}{\omega_B}\frac{\partial V_E}{\partial t}, \tag{5}$$

with $V_E=-cE_r/B$ the $E\times B$ drift velocity, and $\omega_B=eB/mc$ is the cyclotron frequency. The particle motion is described by the following equations:

$$\frac{dv_{||}}{dt}=-\epsilon\frac{v^2-v_{||}^2}{2}\frac{\sin\theta}{qR}+\frac{v_{||}V_E\sin\theta}{R}, \tag{6}$$

$$\frac{dv^2/2}{dt}=-\frac{v_{||}^{2R}+v^2}{2}\sin\theta.V_E. \tag{7}$$

The safety factor is given by $q=\epsilon/\Theta$. We use the standard neoclassical ordering $\rho_i/(\Theta L)\ll 1$, where $\rho_i=v_T/\omega_B$, with the thermal velocity $v_T=(2T/m)^{1/2}$, and L is the characteristic scale of density and temperature variations. We next linearize Eq. (4) by representing f as $f=f_M+\hat{f}$, where the Maxwellian part f_M is given by

$$f_M=n(m/2\pi T)^{3/2}\exp[-mv^2/2T], \tag{8}$$

The equation for $\tilde{f}$ reads:

$$\frac{\partial\tilde{f}}{\partial t}+\frac{v_{||}}{qR}\frac{\partial\tilde{f}}{\partial\theta}-\epsilon\frac{v^2-v_{||}^2}{2}\frac{\sin\theta}{qR}\frac{\partial\tilde{f}}{\partial v_{||}}-St(\tilde{f})=\sin\theta\frac{m(v_{||}^2+v^2)}{2RT}\left[V_E+V_n+\left(\frac{mv^2}{2T}-\frac{3}{2}\right)V_T\right]f_M, \tag{9}$$

where the drift velocities are given by $V_n=cT/(eBL_n)$ and $V_T=cT/eBL_T$. Here $L_n=d\ln n/d\ln r$ and $L_T=d\ln T_i/d\ln r$. Note that we have neglected the electric drift $V_E=(c/B)d\Phi/dr$ in the second term in Eq. (9), since we restrict ourselves only by the case of the ‘‘moderate’’ electric fields, such that $V_E/(\Theta v_T)\ll 1$. Also the polarization drift velocity has been neglected in Eq. (9), which is consistent with the ordering $\rho_i/(\Theta L)\ll 1$.

It is convenient to rewrite Eq. (9) using new variables $z=v_{||}/v$ and v:

$$\frac{\partial\tilde{f}}{\partial t}+\frac{zv}{qR}\frac{\partial\tilde{f}}{\partial\theta}-\epsilon\frac{v(1-z^2)}{2}\frac{\sin\theta}{qR}\frac{\partial\tilde{f}}{\partial z}-St(\tilde{f})=\sin\theta\frac{mv^2(1+z^2)}{2RT}\left[V_E+V_n+\left(\frac{mv^2}{2T}-\frac{3}{2}\right)V_T\right]f_M. \tag{10}$$

Now we specify the collisional operator $St(f)$:

$$St(f)=\nu_c(x)\frac{\partial}{\partial z}(1-z^2)\frac{\partial f}{\partial z}+z\hat{S}_1 f, \tag{11}$$

where $x^2=mv^2/(2T)$, and the function ν_c is

$$\nu_c(x)=\frac{3(2\pi)^{1/2}\nu_{ii}}{4x^3}\left[\left(1-\frac{1}{2x^2}\right)erf(x)+\frac{\exp(-x^2)}{\sqrt{\pi}x}\right], \tag{12}$$

with $\nu_{ii}=4\pi ne^4\lambda/(m^2v_T^3)$ the frequency of the ion–ion collisions, λ the Coulomb logarithm, and *erf*(x) the error function. The operator $\hat{S}_1$ in Eq. (11) is taken to be in the Hirshman–Sigmar–Clarke[32] form:

$$\hat{S}_1 f = 3[\nu_c(x) - \nu_S(x)]\int_{-1}^{1} zf dz$$

$$+3x\nu_S(x) f_M \frac{\int \nu_S(x)x^3\left(\int_{-1}^{1} zf dz\right)dx}{\int \nu_S(x)x^4 f_M dx}, \tag{13}$$

where the "slowing down" frequency $\nu_S(x)$ is given by

$$\nu_S(x) = \frac{2\nu_{ii}}{x^3}\left[\mathrm{erf}(x) - \frac{2x\,\exp(-x^2}{\sqrt{\pi}}\right]. \tag{14}$$

Next we perform a normalization of Eq. (10). We use a time unit, given in terms of the ion transit time $\hat{t} = t v_T/(qR)$, the collisional frequency is normalized in the same way, $\hat{\nu}_c = \nu_c(x) v_T/(qR)$. Finally, the distribution function $\hat{f}$ is normalized in terms of the Maxwellian function f_M: $\tilde{f} = \hat{f} f_M$. Using the above-described normalization Eq. (10) may be written as

$$\frac{\partial \hat{f}}{\partial \hat{t}} + zx\frac{\partial \hat{f}}{\partial \theta} - \epsilon\frac{x(1-z^2)}{2}\sin\,\theta\frac{\partial \hat{f}}{\partial z} - \hat{S}t(\hat{f})$$

$$= \sin\,\theta x^2(1+z^2)\left[\hat{V}_E + \hat{V}_n + \left(x^2 - \frac{3}{2}\right)\hat{V}_T\right], \tag{15}$$

where we have also normalized the drift velocities: $\hat{V}_E = qV_E/v_T, \hat{V}_n = qV_n/v_T$, and $\hat{V}_T = qV_T/v_T$. Note that the "stoss" term in (15) is given by (10),(12) with $\widehat{\nu_{ii}} = \nu_{ii} v_T/(qR)$.

We supplement Eq. (15) by the quasineutrality condition:

$$\langle j_r \rangle = \int R f V_r d^3 v\, d\theta = 0, \tag{16}$$

where the radial drift is given by (5), and $d^3 v = 2\pi v^2 dv\, dz$, such that the integration over x and z are taken from 0 to ∞ and from -1 to 1, respectively. In our normalized units the linearized version of this equation takes a form:

$$\frac{\partial \hat{V}_E}{\partial \hat{t}} + \frac{q^2}{2\pi^{3/2}}\int (1+z^2)x^4\,\exp(-x^2)\hat{f}\,\sin\,\theta dx dz d\theta = 0, \tag{17}$$

where the same integration convention is used.

In the next sections we omit "hats" in Eqs. (15),(17) for simplicity. We are also interested in the poloidally averaged macroscopic parallel velocity. This quantity is given by $\overline{U_{\|}} = \int v_{\|} f d^3 v\, d\theta / (\int f d^3 v\, d\theta)$. Its normalized version $\widehat{\overline{U_{\|}}}$, such that $\widehat{\overline{U_{\|}}} = \epsilon \overline{U_{\|}}/v_T$, is given by:

$$\overline{U_{\|}} = \frac{\epsilon}{\pi^{3/2}}\int x^3 z\,\exp(-x^2) f dx dz d\theta, \tag{18}$$

where we have omitted "hats" in f and $\overline{U_{\|}}$ in Eq. (18). Next we represent $\hat{f}$ in Eq. (15) as

$$\hat{f}(\theta, z, x) = \Sigma F_n(x,\theta) P_n(z), \tag{19}$$

where $n = 0,1,2,\cdots$, and $P_n(z)$ is the Legendre polynomial of the n order (it is instructive to compare with a steady-state solution, obtained by Hinton and Rosenbluth[33]). Using the following recursion properties of the Legendre polynomials:[34]

$$(n+1)P_{n+1} = (2n+1)zP_n - nP_{n-1}, \tag{20}$$

$$(z^2-1)dP_n/dz = nzP_n - nP_{n-1}, \tag{21}$$

we perform the following standard procedure. We substitute (19) into (15), then multiply each of equations by P_n and integrate from -1 to 1. Note that the magnetic drift in the right-hand side of Eq. (15) is proportional to $(4P_0 + 2P_2)/3$. We use the following property of the collisional operator:

$$\hat{S}t(\Sigma B_n(x)P_n) = -\Sigma(\hat{\nu}_n B_n)P_n, \tag{22}$$

where

$$\hat{\nu}_n(x)B_n = n(n+1)[\hat{\nu}_c - \delta_{1,n}(\hat{\nu}_c - \hat{\nu}_S)]B_n$$

$$-x\hat{\nu}_S\delta_{1,n}\frac{\int x^3\hat{\nu}_S B_n dx}{\int x^4\hat{\nu}_S\,\exp(-x^2)dx}, \tag{23}$$

where $\delta_{i,j}$ is the Kronecker symbol, and we use normalized Eqs. (12) and (14) for $\hat{\nu}_c$ and $\hat{\nu}_S$, respectively. Using the integration property $\int P_n P_m dz = \delta_{m,n} 2/(2n+1)$, we eventually come to a system of coupled equations for functions F_n:

$$\frac{\partial F_n}{\partial t} + x\left(\frac{n}{2n-1}\frac{\partial F_{n-1}}{\partial \theta} + \frac{n+1}{2n+3}\frac{\partial F_{n+1}}{\partial \theta}\right)$$

$$+\frac{\epsilon}{2}\sin\,\theta x\left[\frac{n(n-1)}{2n-1}F_{n-1} - \frac{(n+1)(n+2)}{2n+3}F_{n+1}\right]$$

$$+\hat{\nu}_n F_n = x^2\,\sin\,\theta\frac{4\delta_{0,n} + 2\delta_{2,n}}{3}\left[V_E + V_n + \left(x^2 - \frac{3}{2}\right)V_T\right], \tag{24}$$

where $\hat{\nu}_n$ is given by Eq. (24). The supplementary quasineutrality equation has a form:

$$\frac{\partial V_E}{\partial t} + \frac{4q^2}{3\pi^{3/2}}\int (F_0 + 0.1F_2)\sin\,\theta x^4\,\exp(-x^2)dx d\theta = 0. \tag{25}$$

The parallel velocity $\overline{U_{\|}}$ is given here by:

$$\overline{U_{\|}} = \frac{2\epsilon}{3\pi^{3/2}}\int x^3\,\exp(-x^2)F_1 dx d\theta. \tag{26}$$

System (24)–(25) represents our basic equations for the numerical simulation. Equation (24) is also subject to a boundary condition $F_\infty = 0$. For simplicity we neglect the contribution from the electrons. The initial value code "ELECTRIC," developed by us for modeling (24)–(25), uses an operator splitting technique and, accordingly, has a suitable combination of implicit and explicit difference schemes. Typical number of grid points in (x, z, θ) space for very low collisionality like $\hat{\nu} = 0.005$ is $64 \times 128 \times 64$. As it is known from the neoclassical steady-state theory[33] the

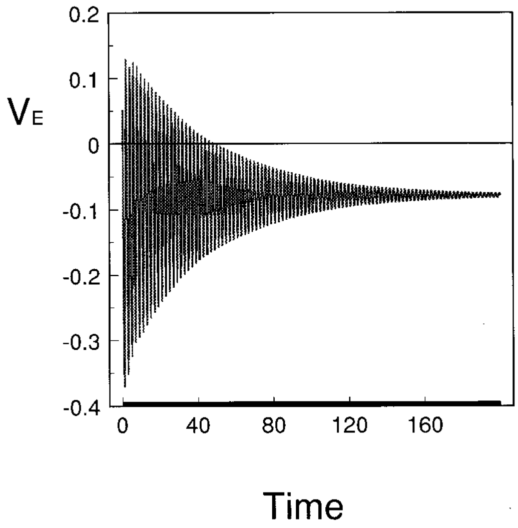

FIG. 1. The electric field drift V_E evolution. The PLATEAU collisional regime with $V_T=0.1, V_n=0.0, \epsilon=0.1, \hat{\nu}=0.1$. Figs. 1 and 2 describes a *non-resonant* situation with $q=3.0$.

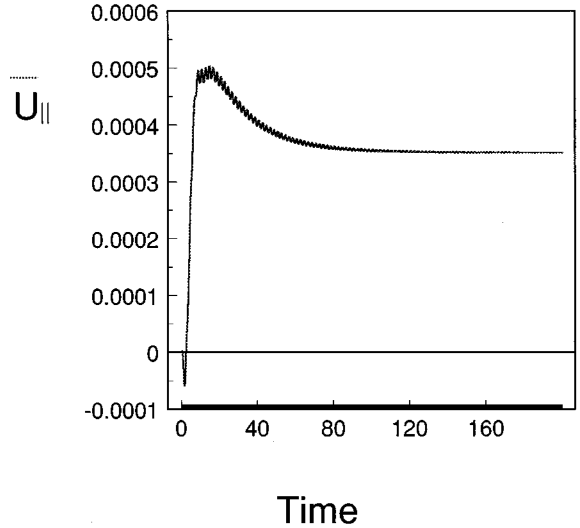

FIG. 2. The parallel velocity evolution. The PLATEAU collisional regime with $V_T=0.1, V_n=0.0, \epsilon=0.1, \hat{\nu}=0.1$.

number of the Legendre polynomials is scaled as $\hat{\nu}^{-1/3}$. This scaling is consistent with our simulation. Every run is characterized by a triad (ϵ, q, ν_*). We note that each of these parameters has a special physical meaning: ϵ controls the mirror force and accordingly the number of bananas, ν_* is the collisionality of plasmas, and q is responsible for the Landau resonance. Thus, each combination provides a unique relaxation scenario. We present the cases for the lower collisional regimes mostly.

III. MODELING OF THE RELAXATION

We start presenting the results of the numerical simulation of Eqs. (24)–(25). As was defined in the Section I, the ''standard'' relaxation scenario corresponds to $F_n(\theta,x,t=0)=0$, where $n=0,1,\cdots$, and $V_E(t=0)=0$. Thus, the initial distribution is a local Maxwellian. Figures 1 and 2 correspond to the plateau collisional regime with $V_T=0.1, V_n=0.0, \epsilon=0.1, \hat{\nu}=0.1$. It is a non-resonant situation with $q=3.0$. Figure 1 shows the electric field drift V_E evolution, and Fig. 2 the parallel velocity, given by Eq. (26). The time unit corresponds to one transit time. One can see the presence of GAM oscillations. Clearly, the damping is of a pure collisional mechanism in this case. The magnitude of the parallel velocity is much smaller than the effective $\mathbf{E}\times\mathbf{B}$ velocity: $|\overline{U_{\|}}| \ll |V_E|$. Figures 3 and 4 differ from Figs. 1 and 2 by one change: $q=1.2$. This is a true ''resonant'' situation. Indeed, the collisionless limit of Ref. 31 provides the oscillation frequency: $\omega_{\rm GAM}^2=7/8q^2$ (see also Section V). Hence, the condition for a particle to be in the resonance with a wave is $q_{res}=(8/7)^{1/2}$. As one expects, in Fig. 3 the GAM oscillations are gone within several transit times. The parallel flow is again very small in this case. In the remainder of this section we do not present the parallel flow, since it was small in all our runs; see, however, Section V, where a relation between V_E and the parallel flow is discussed.

We now consider the banana regime. We start from the same parameters as in the plateau regime, but with $\hat{\nu}=0.02$. This corresponds to $\nu_*=0.63$. Figure 5 corresponds to the non-resonant case with $q=3.0$ (cf. Figs. 1–2). One can see, that the relaxation time is strongly increased, which is apparently related to a smaller collisionality. In Fig. 6 the resonant case $q=1.2$ is plotted. It has similar features as the one in the Fig. 3 in the sense of the rapid damping of the oscillations, within several transit times. One can also see a slow residual relaxation after the oscillations are gone. This is the first evidence of the existence of *another* root in Eq. (3), namely, the collisional magnetic pumping!

We have so far considered the ''standard'' case. The GAM oscillations have always accompanied the relaxation process. How can one extract the information about the mag-

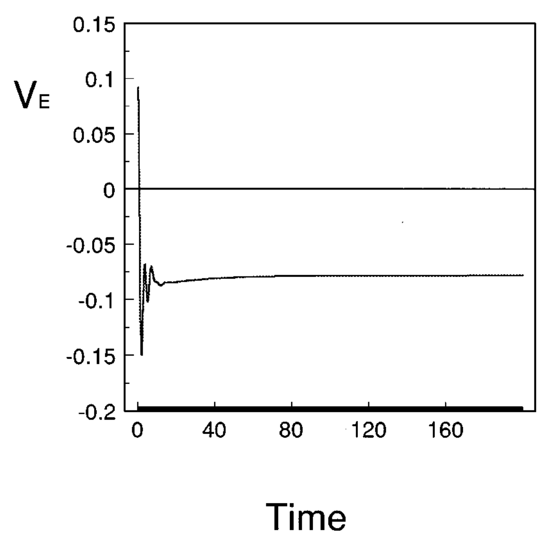

FIG. 3. The electric field drift V_E evolution. The PLATEAU collisional regime with $V_T=0.1, V_n=0.0, \epsilon=0.1, \hat{\nu}=0.1$. Figs. 3 and 4 describes a *resonant* situation with $q=3.0$.

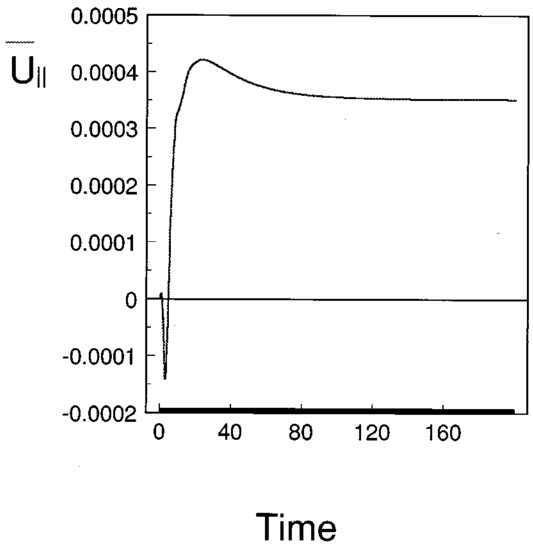

FIG. 4. The parallel velocity evolution. The PLATEAU collisional regime with $V_T=0.1, V_n=0.0, \epsilon=0.1, \hat{\nu}=0.1$.

netic pumping in the system? To answer this question we propose the following numerical experiment. We start from a ''standard' case and reach some steady-state. As we have seen in Figs. 1–6, this usually requires many transit times. Then we slowly change the temperature gradient:

$$V_T = V_{T0} * [1 + \alpha \tanh((t - t_0)/\delta t)], \tag{27}$$

where α is some number, and δt satisfies the condition $\omega_b \delta t \gg 1$, or in our normalizing units $\delta t \gg 1$. Thus, this change is adiabatic in respect to the transit time. At the same time this time should be shorter than τ_R—the collisional relaxation time. For example, in the case of Fig. 3 the relaxation time $\tau_R \approx 100$. Thus, it is sufficient to take $\delta t = 10$. The full run with parameters $V_T(t=0)=0.1, V_n=0.0, \epsilon=0.2,$

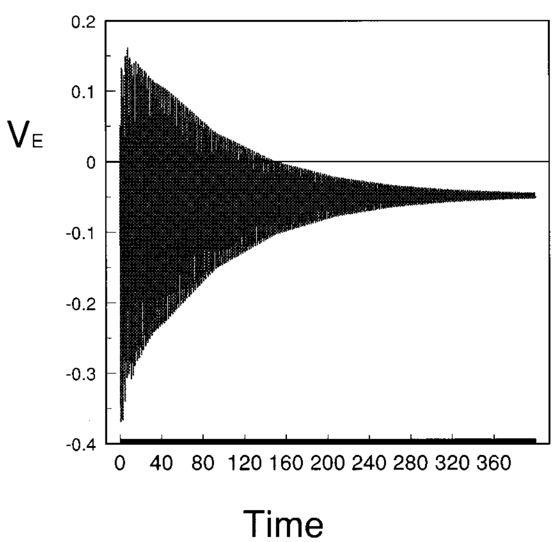

FIG. 5. The electric field drift V_E evolution. The BANANA collisional regime with $V_T=0.1, V_n=0.0, \epsilon=0.1, \hat{\nu}=0.02$. Fig. 5 describes a *non-resonant* situation with $q=3.0$.

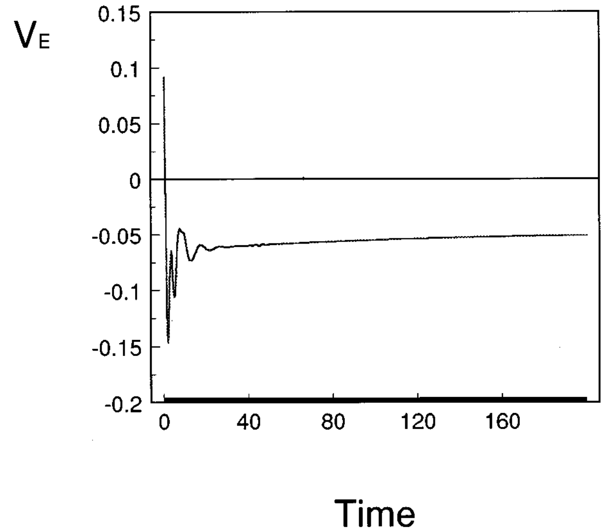

FIG. 6. The electric field drift V_E evolution. The BANANA collisional regime with $V_T=0.1, V_n=0.0, \epsilon=0.1, \hat{\nu}=0.02$. Fig. 6 describes a *resonant* situation with $q=3.0$.

$\hat{\nu}=0.02, q=3.0$ is plotted (in Fig. 9 below). The effective neoclassical parameter $\nu_* = 0.22$, so it corresponds to a ''deep'' banana regime. Here the parameter α in Eq. (27) is taken to be $\alpha = 10$. Since we deal with the linearized system, the value of α is chosen only for better visualization properties. The solid line in Fig. 7 shows the electric field velocity V_E and the dotted line the V_T variation. First, one can see, that during and after the adiabatic change, given by Eq. (27), the GAM oscillations did not take off, as expected. On the other hand, after the switch-on is complete, the system is still far away from the equilibrium. This late stage allows for the exponential fit as in Eq. (2). It provides $\gamma_{MP} = 0.016$ for this case.

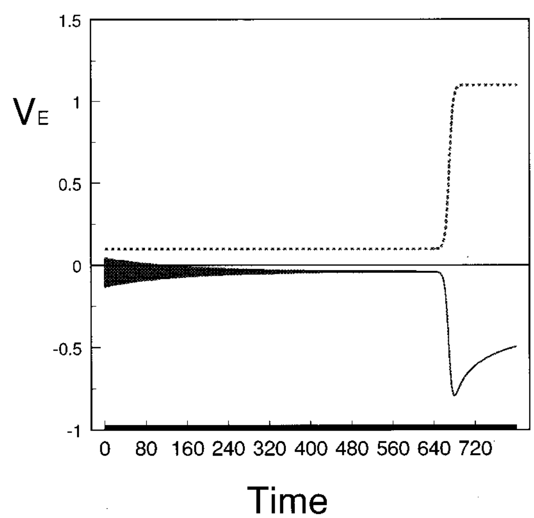

FIG. 7. Relaxation with the adiabatic switch-on of the temperature gradient at the moment $t=640$. The electric field drift V_E is plotted by solid line, the V_T velocity is plotted by the dotted line. The BANANA collisional regime with $V_T=0.1, V_n=0.0, \epsilon=0.1, \hat{\nu}=0.02$, and *non-resonant* $q=3.0$.

It is interesting to consider different values of ϵ, since there has been a lot of controversial results, regarding the ϵ dependence of γ_{MP}. The run with $\epsilon = 0.1$ and the same other parameters as in Fig. 7 yields the relaxation rate for the magnetic pumping $\gamma_{MP} = 0.02$. One can see a substantial change due to ϵ. Qualitatively, the ''soft'' switch-on regime and the consequent magnetic evolution can be understood as follows. In the neoclassical equilibrium the distribution of bananas can be obtained from the solution of the drift kinetic equation

$$zx\frac{\partial \hat{f}}{\partial \theta} - \epsilon \frac{x(1-z^2)}{2} \sin\,\theta \frac{\partial \hat{f}}{\partial z} = \sin\,\theta x^2(1+z^2)\left[\hat{V}_E + \hat{V}_n + \left(x^2 - \frac{3}{2}\right)\hat{V}_T\right]\exp(-x^2), \tag{28}$$

which is just as Eq. (15) with no time derivative and collisional terms, but with the restored exponential factor. This equation corresponds to the ordering $\hat{\nu} \ll \omega_b$ and $\partial/\partial t \ll \omega_b$. It also allows for a slow change in $V_T(t)$ in comparison to the transit time. Equation (28) is the leading order equation of Refs. 22, 25, and 26 (written in a slightly different way). The solution to it, which can be called the banana quasi-steady state, is

$$\hat{f} = -zx(1+\epsilon\,\cos\,\theta)\frac{2}{\epsilon}\left[V_E + V_n + \left(x^2 - \frac{3}{2}\right)V_T\right] \times \exp(-x^2) + C, \tag{29}$$

where C is a function, constant along the field line for given μ and energy, i.e., $C = C(x, \mu(x,z,\theta), E(x,z,\theta))$. It is determined from the solubility condition in the next order in $\hat{\nu}/\omega_b$. However, it is important, that C is zero for the trapped particles because of the parity constraint; see, for example, Ref. 22. Introducing a distribution function $F(z,\theta) = \int \hat{f} x^2 dx$, one obtains from Eq. (29), that $F \sim z(1 + \epsilon\,\cos\,\theta)(V_E + V_n + 0.5V_T)$ for bananas. In a very simplified way the picture of the magnetic pumping looks as follows. After we have adiabatically changed the temperature gradient in accordance with Eq. (28), the bananas, insensitive to collisions, reach their quasi-steady-state within a few bounce periods. For such a short time the distribution of the circulating particles has not changed essentially. Thus, there appears a strong discontinuity at the boundary between the trapped and circulating particles, which yields a friction force ultimately controlling the magnetic pumping phenomena. It then becomes clear, that the magnetic pumping relaxation rate depends on ϵ, since the smoothing of the abovementioned discontinuity happens with the effective collisional frequency ν_{ii}/ϵ.

Let us illustrate the abovementioned qualitative arguments by simulation results, provided by ''ELECTRIC.'' First, we note that the trapping condition for particles at the point θ is $|z| \leq (\epsilon(1+\cos\,\theta))^{1/2}$. We consider three different locations, $\theta = \pi, \theta = 0$, and $\theta = \pi/2$, such that the first location corresponds to the region of the strongest field with no trapped particles, the second, to the weakest magnetic field with a fraction of the trapped particles, given by $|z| \leq (2\epsilon)^{1/2}$, and the third, to the top of the torus, with a fraction of the trapped particles $|z| \leq (\epsilon)^{1/2}$. We present the function $F(z,\theta)$, averaged over one transit time. In Fig. 8 we plot the function F for different locations, such that the curves (1), (2), and (3) correspond to $\theta = \pi, \theta = 0$, and $\theta = \pi/2$, respectively. This is a ''standard'' steady-state case, with parameters $q = 3.0, \epsilon = 0.15, \hat{\nu} = 0.02, V_n = 0.0, V_{T0} = 0.2$. In Fig. 9 the steady-state distribution $F(z, \theta = 0)$ is plotted for two values of collisional frequency, $\hat{\nu} = 0.02$ (solid line), and $\hat{\nu} = 0.01$ (dotted line). One can see that the distribution is close to the linear dependence, given by the integrated Eq. (29), such that the smaller collision frequency is in a better agree-

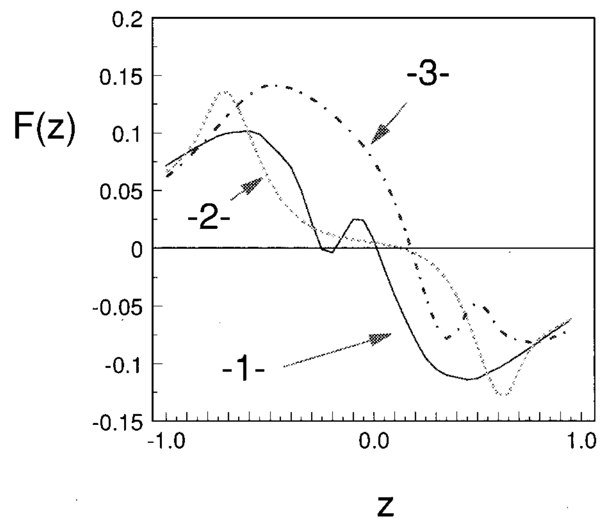

FIG. 8. The steady-state distribution $F(z)$ (integrated over x) vs z at the different poloidal locations. Curves (1), (2), and (3) correspond to $\theta = \pi, \theta = 0$, and $\theta = \pi/2$, respectively. This is the end of the ''standard'' case, with parameters $q = 3.0, \epsilon = 0.15, \hat{\nu} = 0.02, V_n = 0.0, V_{T0} = 0.2$.

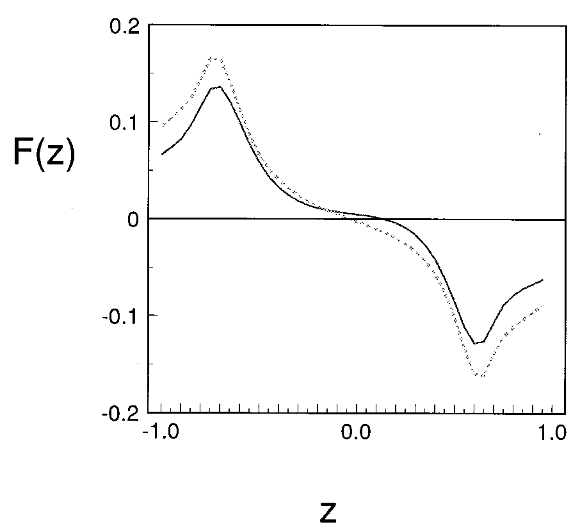

FIG. 9. The steady-state distribution $F(z)$ is plotted for two values of collisional frequency, $\hat{\nu} = 0.02$ (solid line), and $\hat{\nu} = 0.01$ (dotted line). Other parameters are $q = 3.0, \epsilon = 0.15, V_n = 0.0, V_{T0} = 0.2$.

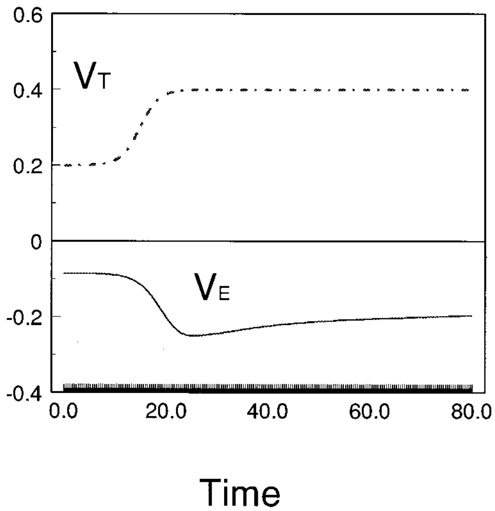

FIG. 10. The case with parameters $q=3.0, \epsilon=0.15, \hat{\nu}=0.02, V_n=0.0$, $V_{T0}=0.2$. The electric field drift V_E is plotted by solid line, the V_T velocity is plotted by the dotted line.

ment. On the other hand, the influence of the boundary layer between the transit and trapped particles is still quite strong, providing a noticeable deviation. Now we perform the adiabatic switch-on, described in detail earlier in this section. We present a case with $\hat{\nu}=0.02$. In Fig. 10 the electric field velocity V_E vs time is plotted. In Fig. 11 the distribution $F(z)$ is plotted at the times $t=0$,40, and 80. One can see, that the magnetic pumping evolution in fact represents a quite complicated behavior. Apart from the dynamics of the transitional layer, there is an evolution of the banana distribution due to varying V_E and V_T. For illustrative purpose we also consider a ''pure'' collisionless case with $\hat{\nu}=0.0$. Namely, on reaching the steady state for $\hat{\nu}=0.02$ we put $\hat{\nu}=0.0$ and perform a usual adiabatic switch-on. In Fig. 12 the distribution $F(z,\theta)$ is plotted at $t=40$. As in Fig. 8 curves (1), (2), and (3) correspond to $\theta=\pi, \theta=0$, and $\theta=\pi/2$, respectively.

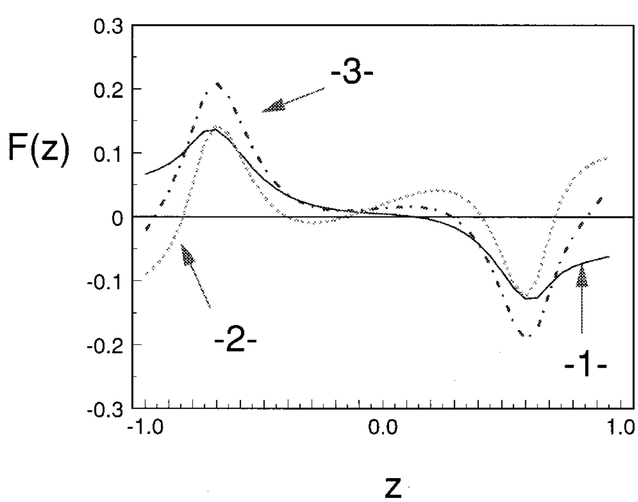

FIG. 11. For the case of Fig. 10 the distribution $F(z,\theta=0)$ is plotted. Curves (1), (2), and (3) correspond to $t=0$,40, and 80, respectively.

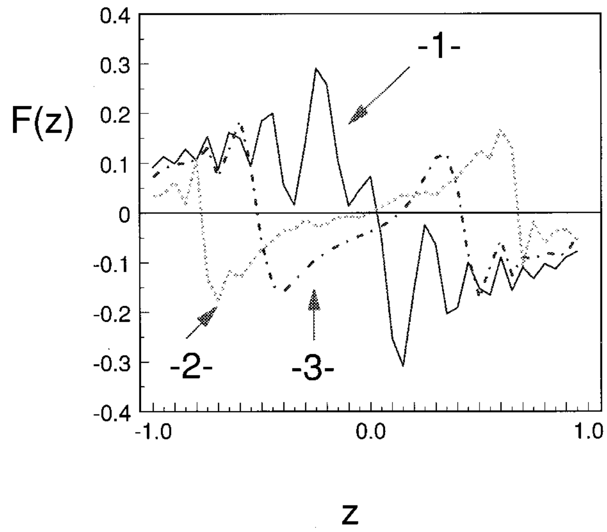

FIG. 12. On reaching the steady-state for $\hat{\nu}=0.02$ the adiabatic switch-on with $\hat{\nu}=0.0$ is performed at $t=0$. The distribution $F(z)$ is plotted at $t=40$. Curves (1), (2), and (3) correspond to $\theta=\pi, \theta=0$, and $\theta=\pi/2$, respectively.

One can see a better agreement with Eq. (29) for the trapped particles in comparison to the finite collision cases. Such simulation allows one to estimate the influence of the boundary layer, since it is known (see, for example, Hinton and Rosenbluth[33]), that solution (29) is not valid there. When ϵ is decreased, the transition from the banana to plateau regime takes place. Namely, all the banana orbits are destroyed when $\epsilon \cong \hat{\nu}^{2/3}$. Then representation like (29) is not possible; all the particles are effected by collisions and participate equally in the formation of the friction force. Thus, there exists a saturation of γ_{MP} in the plateau regime. In Fig. 13 we plot the relaxation rate γ_{MP} vs ϵ for the case $q=3.0, \hat{\nu}=0.015, V_n=0.0, V_{T0}=0.2$. When $\epsilon \rightarrow 0$, and there is no mirror force at all, the only dissipative root in Eq. (3) is γ_{GAM}.

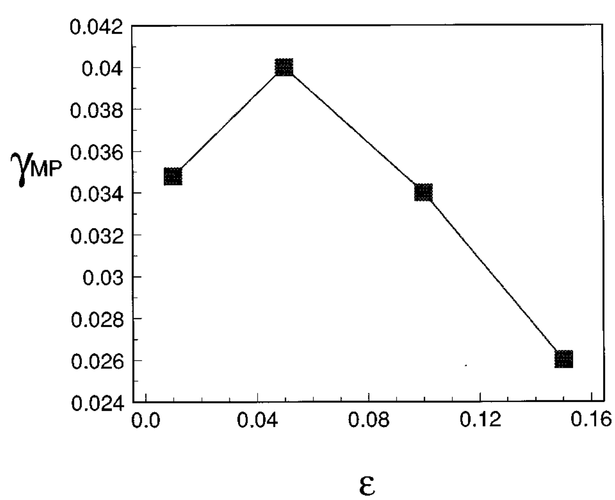

FIG. 13. The relaxation rate of the magnetic pumping γ_{MP} vs ϵ in the banana and plateau regime. Transition from banana to plateau corresponds to $\epsilon=0.061$. Other parameters are $\hat{\nu}=0.02, q=3.0$.

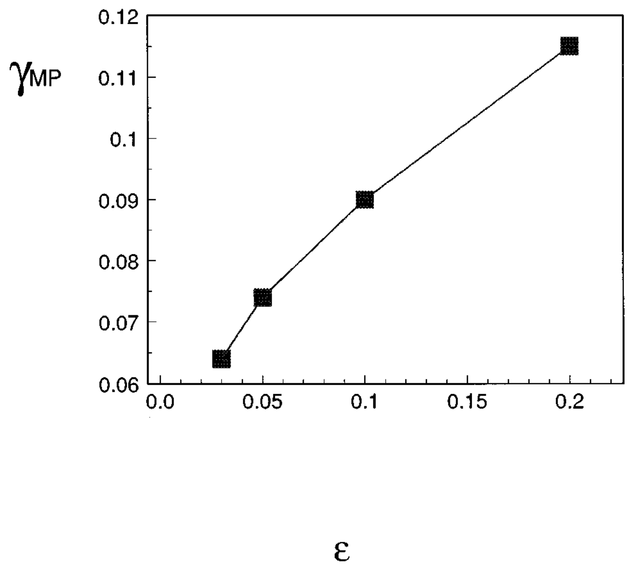

FIG. 14. The relaxation rate of the magnetic pumping γ_{MP} vs ϵ in the plateau regime. Other parameters are $\hat{\nu}=0.25, q=3.0$.

This is consistent with Ref. 31. To illustrate this effect in more detail let us consider the marginal case of $\epsilon=0$. Remarkably, in the absence of the mirror force, there is a collisional damping of the GAM oscillations, but no magnetic pumping at all! It is important, that the region of the inverse dependence γ_{MP} vs ϵ exists only in the banana regime, which is consistent with the qualitative picture, proposed above. In Fig. 14 we plot γ_{MP} vs ϵ for the case $q=3.0, \hat{\nu}=0.25, V_n=0.0, V_{T0}=0.2$. All the points correspond to the plateau regime. One can see, that the magnetic pumping relaxation rate decreases monotonically as ϵ decreases.

IV. FLUID PICTURE OF RELAXATION

It is interesting to consider some general properties of the relaxation, common to all of the collisional regimes. Moreover, a part of this section is devoted to a more general toroidal geometry, rather than the one considered in the previous sections. Namely, we consider an axisymmetric torus, and the magnetic field is given by

$$\mathbf{B}=I\nabla\zeta+\nabla\psi\times\nabla\zeta, \tag{30}$$

where $I=I(\psi)$, and the flux function ψ, toroidal angle ζ, and poloidal angle θ form a coordinate system. Since we are interested in the time-dependent part of velocity only, we use $\mathbf{V}=V_{\|}\mathbf{b}+\mathbf{V_E}$, where $\mathbf{b}=\mathbf{B}/B$. We consider the slow relaxation due to magnetic pumping only. Then, it is possible to use an approximation of the plasma incompressibility, $\nabla\cdot\mathbf{V}=0$, which yields:

$$\mathbf{B}\cdot\nabla\frac{V_{\|}}{B}-c(\nabla\phi\times\mathbf{B})\cdot\nabla\frac{1}{B^2}=0, \tag{31}$$

which can also be presented as

$$\mathbf{B}\cdot\nabla\left(\frac{V_{\|}}{B}-\frac{cI\phi'}{B^2}\right)=0, \tag{32}$$

where we consider $\phi=\phi(\psi)$, and $\phi'=d\phi/d\psi$. Equation (32) yields:

$$\frac{V_{\|}}{B}-\frac{cI\phi'}{B^2}=A(\psi), \tag{33}$$

where A is the integration constant, similar to the one, used by Callen and Shaing.[35] We next consider the equation of motion, given by

$$\rho\frac{d\mathbf{V}}{dt}=-\nabla p+\frac{1}{c}\mathbf{j}\times\mathbf{B}-\nabla\boldsymbol{\pi}, \tag{34}$$

where the viscosity tensor is $\boldsymbol{\pi}=p_\perp\hat{\mathbf{I}}+(p_{\|}-p_\perp)\mathbf{bb}$. Note, that the quasineutrality condition $\nabla\cdot\mathbf{j}=0$ yields

$$\frac{\partial}{\partial\psi}\sqrt{g}j^\psi+\frac{\partial}{\partial\theta}\sqrt{g}j^\theta=0, \tag{35}$$

where $\sqrt{g}$ is the Jacobian, and j^ψ and j^θ are the contravariant components of $\mathbf{j}$. Integrating Eq. (35) over θ one obtains $\langle j^\psi\rangle=0$, where the average over magnetic surface is given by $\langle\ldots\rangle=\int(\ldots)\sqrt{g}d\theta$. This condition was used by Rosenbluth and Taylor.[36] Multiplying Eq. (34) by $\nabla\zeta$ and R^2, the later being $R^2\equiv1/(\nabla\zeta)^2$, one derives a fluid form of the generalized toroidal momentum conservation:

$$\frac{\partial}{\partial t}\langle R^2V^\zeta\rangle=0, \tag{36}$$

where V^ζ is the contravariant component of $\mathbf{V}$. Using the expression for $\mathbf{V}$ one obtains

$$R^2V^\zeta\equiv\mathbf{V}\cdot\nabla\zeta=\frac{V_{\|}I}{B}+\frac{c\phi'}{B^2}(\nabla\psi)^2, \tag{37}$$

Now, combining Eqs. (33), (36), and (37), one obtains a relation between time derivatives of ϕ' and A:

$$c\langle R^2\rangle\frac{\partial\phi'}{\partial t}+I\frac{\partial A}{\partial t}=0. \tag{38}$$

Multiplying Eq. (33) by B^2, differentiating the result in time, and performing the surface averaging we get:

$$\frac{\partial}{\partial t}\langle V_{\|}B\rangle=\langle B^2\rangle\frac{\partial A}{\partial t}+cI\frac{\partial\phi'}{\partial t}. \tag{39}$$

Substituting Eq. (38) into Eq. (39) one obtains the relation between $V_{\|}$ and ϕ' time evolutions:

$$\frac{\partial}{\partial t}\langle V_{\|}B\rangle=cI\frac{\partial\phi'}{\partial t}\left(1-\frac{\langle B^2\rangle\langle R^2\rangle}{I^2}\right). \tag{40}$$

In approximation $B^2\cong I^2/R^2$ we get instead of (40):

$$\frac{\partial}{\partial t}\langle V_{\|}B\rangle=cI\frac{\partial\phi'}{\partial t}\left(1-\left\langle\frac{1}{R^2}\right\rangle\langle R^2\rangle\right). \tag{41}$$

Let us estimate the toroidal relaxation given by Eq. (41) in the low aspect ration approximation. We have

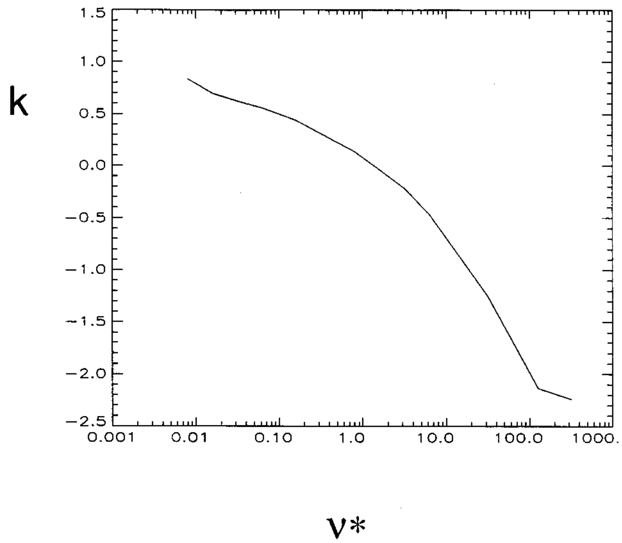

FIG. 15. The Hazeltine parameter k (defined in the Introduction) vs collisionality.

$$cI\phi' \cong cBR\frac{\partial\phi}{\partial r}\frac{1}{\partial\psi/\partial r} \cong \frac{c}{\Theta}\frac{\partial\phi}{\partial r}. \tag{42}$$

Using $1-\langle 1/R^2\rangle\langle R^2\rangle = O(\epsilon^2)$, one obtains

$$\frac{\partial\Theta V_{||}}{\partial t} = O(\epsilon^2)\frac{\partial V_E}{\partial t}. \tag{43}$$

Integration of Eq. (43) with our ''standard'' initial conditions $V_E(t=0)=0$, and $U_{||}(t=0)=0$, yields $\Theta U_{||}(t=\infty) = O(\epsilon^2)V_E(t=\infty)$. This explains the results of Figs. 1–11, that the toroidal velocity is much smaller than V_E. Thus, in accordance to (43) and the formula for the steady-state poloidal velocity, given in the Introduction, in the ''standard'' situation $V_E(t=\infty) \cong (k-1)V_T - V_n$.

To test the results of this section we studied the dependence of the steady state V_E velocity on collisionality with the help of ''ELECTRIC.'' In these runs we performed the adiabatic switch-on of V_T from the very beginning (starting from $V_T=0$) to avoid GAMs and to insure the zero initial values for V_E and $U_{||}$. In Fig. 15 we plot $k \equiv (V_E + V_T + \Theta U_{||})/V_T$ vs collisionality. The parameter k is just the Hazeltine parameter (see Introduction). One can see a good quantitative agreement with analytical values $k(0)=1.17$ and $k(\infty)=-2.1$. At the same time in all of these runs the equilibrium parallel velocity satisfied the relation $\Theta U_{||} = O(\epsilon^2)V_E$.

V. DAMPING OF GAM OSCILLATIONS

In this section we consider the damping of the GAM oscillations. The theory of the Landau damping of them has been proposed by Lebedev *et al.*[31] When the resonant condition is not satisfied, and the Landau damping is exponentially small, we are left with the collisional damping. The technique to determine γ_{GAM} in Eq. (3) has already been pointed out in Ref. 31. Here we present the calculations for the purpose of completeness. For simplicity we consider $V_T = V_n = 0$ in this section. Let us start from the Laplas transform of Eq. (15):

$$pf + zx\frac{\partial f}{\partial\theta} - \epsilon\frac{x(1-z^2)}{2}\sin\theta\frac{\partial f}{\partial z} - \hat{S}t(f) = \sin\theta x^2(1+z^2)V_E. \tag{44}$$

We solve Eq. (44) by perturbations, considering $p \gg 1$. Then,

$$f_1 = \frac{\sin\theta}{p}x^2(1+z^2)V_E, \tag{45}$$

$$pf_2 + zx\frac{\partial f_1}{\partial\theta} - \epsilon\frac{x(1-z^2)}{2}\sin\theta\frac{\partial f_1}{\partial z} - \hat{S}t(f_1) = 0, \tag{46}$$

which yields

$$f_2 = \frac{\sin\theta}{p^2}V_E x^2 \nu_c(x)(2-6z^2), \tag{47}$$

where $\nu_c(x)$ is given by Eq. (12). Substituting Eq. (47) into Eq. (17) one obtains:

$$p + \frac{q^2}{4p\pi^{1/2}}\int x^6(1+z^2)^2\exp(-x^2)dx\,dz + \frac{q^2}{4p^2\pi^{1/2}}\int x^6(1+z^2)(2-6z^2) \times\exp(-x^2)\nu_c(x)dx\,dz = 0. \tag{48}$$

Performing the integration in Eq. (48) we get the dispersion relation for GAMs:

$$p^2 + \frac{7q^2}{8} - \frac{\nu_{ii}q^2}{p} = 0, \tag{49}$$

which yields the collisional damping of GAMs: $\gamma_{\mathrm{GAM}} \cong 4\nu_{ii}/(7q)$. There is no ϵ dependence here. Physically this is because the GAMs are not sensitive to details of the banana distribution.

VI. CONCLUSION

We have considered the time evolution of the radial electric field in the neoclassical plasmas. It has been shown that typically the relaxation is accompanied by the geodesic acoustic mode (GAM) oscillations as well as the magnetic pumping. We have distinguished the slow magnetic pumping relaxation from the GAM oscillations in low collisional plasmas. The GAMs have their own relaxation, sensitive to the Landau resonance condition. This condition, written in terms of the plasma safety factor q, is $q \cong 1.2$. If it is satisfied then there is a strong Landau damping of GAM oscillations, whereas for $q \gg 1$ there exists only the slow collisional relaxation with $\gamma_{\mathrm{GAM}} \cong \nu_{ii}$. By performing a ''soft'' switch-on of the ion temperature gradient we have been able to separate GAM oscillations from the slower magnetic pumping relaxation. It has its own relaxation rate, sensitive to the mirror force strength. As far as the ϵ dependence is concerned our results are qualitatively consistent with predictions by Taguchi,[24] Hsu *et al.*,[25] Novakovskii *et al.*,[26] and Galeev *et al.*,[27] that γ_{MP} is inversely proportional to ϵ. The exact scaling index (if exists!) is hard to extract even in the region of very low collisions. We have studied the plateau regime too, where the magnetic pumping relaxation rate decreases monotonically as ϵ decreases. We have also developed a fluid approach for calculating the $\mathbf{E}\times\mathbf{B}$ and toroidal flow relaxation. We have found that typically the relaxation of the parallel flow is weaker than the V_E relaxation; see Eq. (43). Thus, the net poloidal flow consists primarily of the $\mathbf{E}\times\mathbf{B}$ and the diamagnetic drifts. These general analytical results are consistent with our numerical simulation.

Finally we would like to discuss possible practical implications of the obtained results. We see three problems, where they can be relevant. The first one is related to the equilibrium $\mathbf{E}\times\mathbf{B}$. We have shown in Section IV that in some simple situations (most notably in the absence of large toroidal flows) there exists a functional dependence V_E vs the pressure gradient given by Fig. 15. This can be useful in analysis of the H-mode, where the level of fluctuations is small, theory of Sections II–IV can be applicable, and the complete radial profile of E_r can be reconstructed. Second, we have shown that the relaxation takes place on the scales of the ion–ion collisional time. For typical DIII-D-like core parameters $n=10^{14}\text{cm}^{-3}, T_i=10\text{ keV}$, $R=160$ cm, this yields $\tau_{rel}\approx 10^{-2}$ s. This is consistent with the time of the L-H transition,[4] thus the mechanism described in the paper can be important for understanding of the $\mathbf{E}\times\mathbf{B}$ flow generation. Third, the quantitative information about the magnetic pumping rate can be useful for analytical and numerical models of L-H transitions (see, for example, Ref. 9), where the H-mode threshold is obtained as a balance between the turbulent drive and the magnetic pumping.

ACKNOWLEDGMENTS

S. V. Novakovskii would like to thank T. M. Antonsen, A. A. Galeev, A. B. Hassam, V. B. Lebedev, and P. N. Yushmanov for attention to the paper and many fruitful discussions.

The work was supported by the U.S. Department of Energy.

[1] F. Wagner, G. Becker, K. Behringer, D. Campbell, A. Eberhagen, W. Engelhardt, G. Fussmann, O. Gehre, J. Gernhardt, G. v. Gierke, G. Haas, M. Huang, F. Karger, M. Keilhacker, O. Klueber, M. Kornherr, K. Lackner, G. Lisitano, G. G. Lister, H. M. Mayer, D. Meisel, E. R. Mueller, H. Murmann, H. Niedermeyer, W. Poschenrieder, H. Rapp, H. Rohr, F. Schneider, G. Siller, E. Speth, A. Staebler, K. H. Steuer, G. Venus, O. Vollmer, and Z. Yue, Phys. Rev. Lett. **49**, 1408 (1982).

[2] F. Levington, M. Zarnstorf, S. H. Batha, M. Bell, R. E. Bell, R. V. Budny, C. Bush, Z. Chang, E. Fredrickson, A. Janos, J. Manickam, A. Ramsey, S. A. Sabbagh, G. L. Schmidt, E. J. Synakowski, and G. Taylor, Phys. Rev. Lett. **75**, 4417 (1995); for general information on TFTR see D. J. Grove and D. M. Meade, Nucl. Fusion **25**, 1167 (1985).

[3] E. J. Strait, L. L. Lao, M. E. Mauel, B. W. Rice, T. S. Taylor, K. H. Burrell, M. S. Chu, E. A. Lazarus, T. H. Osborne, S. J. Thompson, and A. D. Turnbull, Phys. Rev. Lett. **75**, 4421 (1995).

[4] K. H. Burrell, Phys. Plasmas **4**, 1499 (1997); for general information on DII-D see J. L. Luxon and L. G. Davis, Fusion Technol. **8**, 441 (1985).

[5] H. Biglary, P. H. Diamond, and P. W. Terry, Phys. Fluids B **2**, 1 (1990).

[6] P. Diamond and Y. B. Kim, Phys. Fluids B **3**, 1626 (1991).

[7] K. S. Shaing and E. C. Grume, Phys. Rev. Lett. **63**, 2369 (1989).

[8] T. Stringer, Phys. Rev. Lett. **22**, 770 (1969).

[9] A. B. Hassam, T. M. Antonsen, J. F. Drake, and C. S. Liu, Phys. Rev. Lett. **66**, 309 (1991).

[10] R. Z. Sagdeev and A. A. Galeev, Dokl. Akad. Nauk SSSR **189**, 1204 (1969) [Sov. Phys. Dokl. **14**, 1198 (1970)].

[11] S. P. Hirshman, Nucl. Fusion **18**, 917 (1978).

[12] A. A. Galeev and R. Z. Sagdeev, Sov. Phys. JETP **26**, 233 (1968).

[13] A. A. Galeev, Sov. Phys. JETP **32**, 752 (1971).

[14] S. P. Hirschman and D. J. Sigmar, Nucl. Fusion **21**, 1079 (1981).

[15] F. L. Hinton and R. D. Hazeltine, Rev. Mod. Phys. **48**, 239 (1981).

[16] M. N. Rosenbluth, P. H. Rutherford, J. B. Taylor, E. A. Frieman, and L. M. Kovrizhnikh, in *Plasma Physics and Controlled Nuclear Fusion Research, 1970* (International Atomic Energy Agency, Vienna, 1971), Vol. 1, p. 495.

[17] R. D. Hazeltine, Phys. Fluids **17**, 961 (1974).

[18] T. H. Stix, Phys. Fluids **16**, 1260 (1973).

[19] T. E. Stringer, J. Plasma Phys. **10**, 433 (1973).

[20] M. N. Rosenbluth, Bull. Am. Phys. Soc. **18**, 1337 (1973).

[21] K. C. Shaing and S. P. Hirshman, Phys. Fluids B **1**, 705 (1989).

[22] A. B. Hassam and R. M. Kulsrud, Phys. Fluids **21**, 2271 (1978).

[23] M. Taguchi, Plasma Phys. Controlled Fusion **30**, 1897 (1988).

[24] M. Taguchi, Plasma Phys. Controlled Fusion **33**, 859 (1991).

[25] C. T. Hsu, K. C. Shaing, and R. Gormley, Phys. Plasmas **1**, 132 (1994).

[26] S. V. Novakovskii, A. A. Galeev, C. S. Liu, R. Z. Sagdeev, and A. B. Hassam, Phys. Plasmas **2**, 3566 (1995).

[27] A. A. Galeev, R. Z. Sagdeev, C. S. Liu, and S. V. Novakovskii, JETP **82**, 875 (1996).

[28] R. C. Morris, M. G. Haines, and R. J. Hastie, Phys. Plasmas **3**, 4513 (1996).

[29] N. Winsor, J. L. Johnson, and J. M. Dawson, Phys. Fluids **11**, 2448 (1968).

[30] A. B. Hassam and J. F. Drake, Phys. Fluids B **5**, 4022 (1993).

[31] V. B. Lebedev, P. N. Yushmanov, P. H. Diamond, S. V. Novakovskii, and A. I. Smolyakov, Phys. Plasmas **3**, 3023 (1996).

[32] S. P. Hirshman, D. J. Sigmar, and J. F. Clarke, Phys. Fluids **19**, 656 (1976).

[33] F. L. Hinton and M. N. Rosenbluth, Phys. Fluids **16**, 836 (1973).

[34] M. Abramowitz and I. Stegun, *Handbook of Mathematical Functions* (Dover, New York, 1970), p. 332.

[35] J. Callen and K. C. Shaing, Phys. Fluids B **5**, 4022 (1985).

[36] M. N. Rosenbluth and J. B. Taylor, Phys. Rev. Lett. **66**, 309 (1969).